Cement and Concrete Composites 83 (2017) 415–426

Contents lists available at ScienceDirect

Cement and Concrete Composites

journal homepage: www.elsevier.com/locate/cemconcomp

Accelerated microwave curing of concrete: A design and performance-related experiments

Natt Makul [a, *], Phadungsak Rattanadecho [b], Amphol Pichaicherd [b]

[a] Department of Building Technology, Faculty of Industrial Technology, Phranakhon Rajabhat University, Changwattana Road, Bangkhen, Bangkok 10220, Thailand

[b] Center of Excellence in Electromagnetic Energy Utilization in Engineering (CEEE), Department of Mechanical Engineering, Faculty of Engineering, Thammasat University Prathum Thani, 12121, Thailand

ARTICLE INFO

Article history:
Received 11 December 2015
Received in revised form
22 June 2017
Accepted 8 August 2017
Available online 16 August 2017

Keywords:
Microwave
Concrete
Curing
Prototype design
Compressive strength: volume stability

ABSTRACT

Microwave (MW)-accelerated curing has emerged as an innovative and popular curing method for concrete materials. This paper reports the results of a study to model the horn antenna used for the MW irradiation of a workpiece with a mobile MW-accelerated concrete curing unit, based on a coupled thermal and electromagnetic analysis. The mathematical models were useful for evaluating the heat generation within a horn antenna and as a basis for constructing a mobile MW-accelerated curing unit with an operating frequency of 2.45 GHz and a MW power level of 800 W. Further, the early-age compressive strength development and volume stability of MW-cured concrete were investigated in terms of its shrinkage and compared to the properties of autoclave-cured concrete. The design results showed that under the concept of the allowable maximum temperature for the concrete workpiece, which was controlled to less than 80 °C, a horn antenna that was 216.70 mm wide, 333.68 mm long, and 273.0 mm high produced a uniform thermal distribution in a concrete workpiece. Moreover, experimental investigations showed that the application period for curing using a mobile MW-curing unit was considerably shorter than that in autoclave curing methods. The appropriate delay time (time after concrete mixing) was 30 min, and MW irradiation for 45 min could improve the maximum 8-h early-age compressive strength of MW-cured concrete, whereas an application time of 15 min produced the 28-day compressive strength. When a concrete workpiece was cured at high temperature using MW energy for more than 15 min at a temperature greater than 80 °C, the effect was a continuous increase in the early-age compressive strength, which was greater than that achieved by autoclave curing. In terms of volumetric stability, MW-curing for 30 and 45 min increased the ultimate shrinkage to a greater extent than that by autoclave curing and vice versa in the case of a MW application time of 15 min.

1. Introduction

Methods of heating, drying, and thawing using MW energy are continuously being developed as innovative and versatile methods for heat processing of dielectric materials. In particular, operating frequencies of 0.915 ± 0.013 GHz and 2.45 ± 0.05 GHz—the two principal MW frequencies assigned by the International Microwave Power Institute (IMPI)—are most often used for industrial, scientific, and medical (ISM) purposes [1]. Nowadays, MWs have been widely used in high-temperature industrial processes involving chemical reactions [2–4], wood products [5,6], foodstuffs [7–10], ceramics [11,12], and biological organisms [13,14]. MW processing involves volumetric (bulk) rapid heating and dipole polarization and depolarization of a dielectric material. The interactions instantaneously convert electromagnetic radiation to thermal (heat) energy [1]. One possible application of MW energy is to use MW for the accelerated curing of early-age concrete materials [15–18].

MW energy can be applied to concrete materials. In particular, at room temperature, the loss factor of water, which is a main component of concrete and reacts with cement particles during a hydration reaction, is higher than that of the cement and aggregates. Consequently, when water molecules are irradiated by an electromagnetic wave, energy is transferred and converted from that field to the molecular bonds in water via friction among the negative and positive ions in compressed (dipole polarization) and

* Corresponding author.
E-mail address: shinomomo7@gmail.com (N. Makul).

http://dx.doi.org/10.1016/j.cemconcomp.2017.08.007
0958-9465/

uncompressed (de-polarization) interactions [1]. Therefore, any heat that is generated is dissipated within the concrete being processed, and the temperature of the concrete is monotonically raised. Therefore, an accelerated hydration reaction takes place. Water molecules exist inside the concrete structure before the cement hardens, which can collapse the capillary pores and produce a densified internal concrete structure. Thus, the early-age compressive strength development of the concrete significantly increases, which is a primary goal in the development of concrete for contemporary use [19–22].

2. Fundamental and proposed concepts for MW curing of concrete

The term *MW heating* is equally applicable to both the fundamental and proposed concepts for MW systems. In both cases, the heating is due to the fact that a dielectric material is placed in a high-frequency electric field. The root-mean-square value of the electric field intensity $\vec{E}$ is normally used to evaluate the MW energy absorbed. Based on Lambert's law, the MW energy absorbed can be defined using Eq. (1).

$$Q = \sigma\left|\vec{E}\right|^2 = 2\pi f\varepsilon_0\varepsilon_r'(\tan\delta)E^2, \quad (1)$$

where Q is the MW energy, σ is the effective conductivity, f is the frequency, ε_0 is the permittivity (dielectric constant) of free space (8.8514×10^{-12} F/meter), ε_r' is the relative dielectric constant, tan δ is the loss tangent coefficient, and $\vec{E}$ is the electric field intensity.

When MW energy travels into the dielectric material, its field strength or power intensity (magnitude) attenuates exponentially; this occurs because MW energy is absorbed into dielectric materials and is changed into heat.

It is well known that high-temperature thermal curing methods have an adverse effect on the properties of concrete, both at an early age and in the long term. Therefore, a crucial question arises: Can the MW heating method be effectively applied in the concrete industry? To understand the relationship between the dielectric properties, heat generation, and heat transfer and to determine the high performance concrete characteristics, the parameters for the MW processing of high performance concrete are determined based on its hydration reaction, which comprises three main periods: the early period, middle period, and late period:

- Period 1: The early period, which is also referred to as the dormant period, begins with contact between the cement grains and the water molecules and is characterized by the addition of water. In this period, calcium silicates quickly react to liberate hydroxide ions and heat. In this first (dormant) period, the delay time (the time between the mixing of the cement and water and the application of MW energy) is considered [23,24].
- Period 2: The accelerated or middle period begins with the formation of calcium and hydroxide ions until the system is saturated. Once the system becomes saturated, the calcium hydroxide begins to crystallize. Simultaneously, calcium silicate hydrate (C-S-H) begins to form. The kinetics of the reaction are controlled by the rate at which water molecules diffuse through the C-S-H coating [15].
- Period 3: The final period is referred to as the decelerated or late period. In this period, hydrate products slowly begin to form and continue to form as long as both water and unhydrated silicates are present.

As previously noted, it may be inductively concluded that period 1 (early period) includes a suitable delay time before the MW-curing of concrete. This is because during period 1, the system contains both water molecules and cement, which continue to react with each other. Conversely, during periods 2 and 3, the internal structures have formed, and introducing MW to the concrete in these stages may destroy the formed structures and affect the long-term strength and volume stability [25,26].

To investigate the suitability of using MW to cure concrete, the present research focused on the design of a portable prototype based on the results of coupled thermal and electromagnetic analyses. The results of experimental investigations on the early-age compressive strength development and volume stability are reported and compared with those for conventional autoclave curing in terms of the shrinkage.

3. Design of horn antenna using 3D mathematical models

Hot spots are undesirable in a concrete material because they can cause the internal structure to crack, thus undermining the performance of the concrete and rendering the concrete less durable. In particular, these can form when curing at a high temperature of more than 80 °C, as a result of the occurrence of delayed ettringite formation (DEF), which is often found in concrete subjected to high-temperature curing [27–30]. Further, to produce uniform electromagnetic heating, various MW systems have been developed with different heating (thermal) distributions by changing the MW feeding system and horn antenna. Some ideas have been developed regarding empty cavities; nevertheless, these do not work under practical conditions [31]. In one analysis, COMSOL Multiphysics Modeling software [32–34] was utilized to construct a horn antenna model based on the finite element method (FEM), to determine the distributions of generated modes and the electric field strength.

The design process is shown in Fig. 1. The study focused on a horn antenna, and a mathematical model was used to analyze and determine the horn size and configuration based on coupled thermal and electromagnetic analyses with a load (concrete

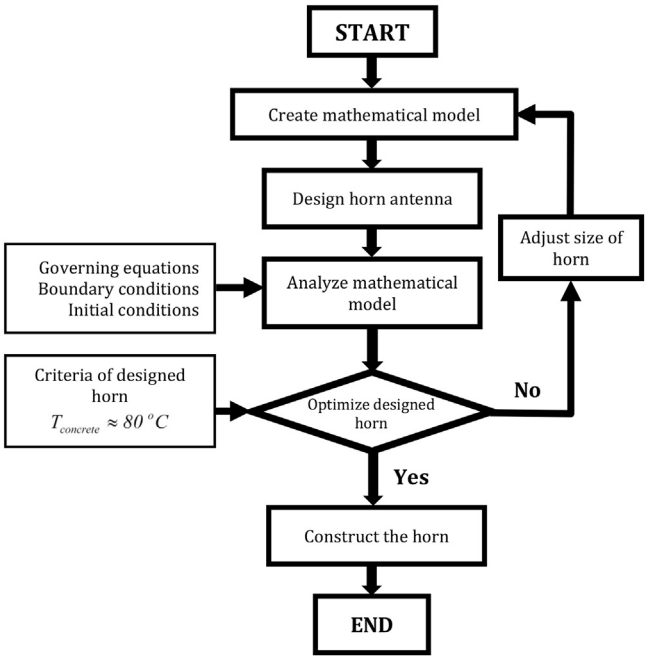

Fig. 1. Horn design process.

workpiece). A 3D mathematical model was considered and analyzed by using COMSOL Multiphysics [32]. The designed horn (width: 216.70 mm, length: 333.68 mm, height: 273.0 mm) was optimized by using the parameters shown in Table 1, under the assumption that the maximum temperature within the concrete workpiece did not exceed 80 °C for MW curing at 2.45 GHz for 15 min. Then, a mobile MW-curing prototype was constructed.

3.1. Mathematical model of horn antenna

To investigate a horn antenna, a mathematical model was applied to determine the design size of the horn and analyze the temperature distribution within a concrete workpiece. In this study, COMSOL™ Multiphysics [32] was used to create the mathematical model, beginning by calculating the designed horn size. Then, the mathematical model was used to analyze and determine the optimal horn size before the horn was constructed.

The mathematical model analysis was divided into two parts: an analysis of the electromagnetic field distribution in the horn and an analysis of the thermal distribution in the concrete. The physical domain is presented in Fig. 2, with the following MW characteristics:

- The waveguide boundaries are perfect electric conductor (PEC).
- The designed horn walls behave like perfect conductors.
- The concrete workpiece is non-magnetic and responds only to the electric field.

3.2. Electromagnetic field and heat generation in horn antenna

The distribution of the electromagnetic field in the horn antenna (in terms of the waveguide, horn antenna, and load) could be determined using Maxwell's electromagnetic field equation [35,36].

Maxwell's equation coupled with the heating model in this study was designed to analyze only the thermal distribution in the concrete workpiece under the electromagnetic field in the horn. According to the assumption that the air in the horn cannot absorb MW energy and transform it into heat, the internal concrete workpiece can transfer heat by conduction, and the load can generate internal heat by transforming the MW energy into heat. Based on this assumption, the heat-exchange equation can be written based on the background from the COMSOL™ Multiphysics program [32] with the conduction mode of heat transfer as Eq. (2):

$$\rho C_p \frac{\partial T}{\partial t} + \nabla \cdot (-k \nabla T) = Q, \tag{2}$$

Table 1
Input parameters for analyzing mathematical model.

Parameters	Value	Unit	Ref.
ε_r	10.25	–	[Measured by Authors]
c_p	880	J/kg.K	[Measured by Authors]
ρ	2300	kg/m^3	[Measured by Authors]
k	1.87	w/m.K	–
Microwave power	800	W	–
f	2.45	GHz	–
t	900	s	–
ε_0	8.85419×10^{-12}	F/m	–
μ_0	$4\pi \times 10^{-7}$	H/m	–
$T(t_0)$	298.15	K	–
ε''_r	0.462	–	[Measured by Authors]
σ	0.964	mho/m	[Measured by Authors]

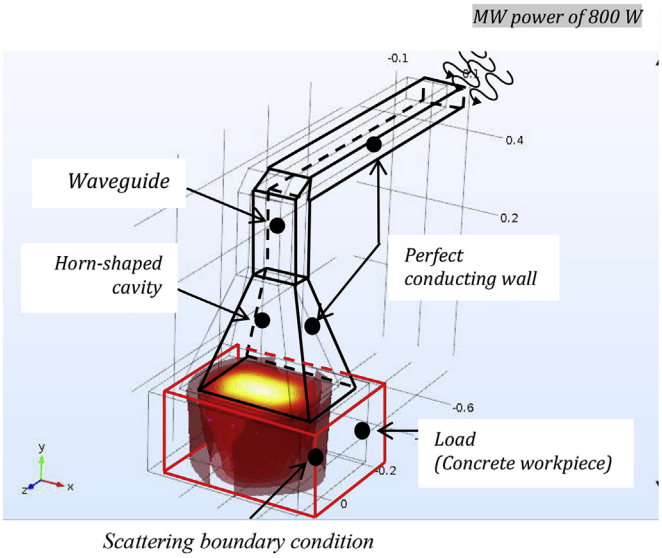

Fig. 2. Physical domain for analyses of electromagnetic field in horn and thermal distribution in concrete workpiece.

where T is the temperature (°C), t is the time (s), C_p is the heat capacity at a constant pressure (J/kg.K), ρ is the density (kg/m^3), k is the thermal conductivity (W/m.K), and Q is the local volumetric heat generation term generated by the absorption of the MW energy (W/M^3).

The scattering boundary condition was applied to the external sides of the calculated domain (i.e., free space) to prevent backward reflection of the outgoing MW from the exterior boundary of the horn-antenna domain, as expressed in Eq. (3):

$$n \times (\nabla \times E) - jkn \times (E \times n) = -n(E_0 \times Jk(n-k))(\exp(-Jk \cdot r)) \tag{3}$$

Heat could only be generated by the load or concrete; therefore, in terms of the heat, the considered domain was focused directly on the load. Thus, the boundary condition for the heat occurred only on the top and wall surfaces of the load (the wall of the load was an insulator, which could not transmit heat).

The boundary condition for heat surfaces at the top and walls of the load (concrete workpiece) is expressed in Eq. (4):

$$n \cdot (-k \nabla T) = 0 \tag{4}$$

The analysis of Maxwell's equation coupled with the heating model of the horn antenna consists of two parts: an analysis of the thermal distribution of the concrete workpiece. Time does not affect the distribution of the electromagnetic field surrounding the concrete workpiece in this analysis, but time does affect the distribution of the electromagnetic field surrounding the concrete workpiece. Thus, this is a transient problem. Therefore, an analysis of the 3D distribution of the electromagnetic field surrounding the concrete workpiece was performed using the COMSOL™ Multiphysics software [32].

In the analysis of the thermal distribution in the concrete, it was found that time had a direct effect on the temperature of the concrete workpiece. This problem was identified as a transient condition. Therefore, an analysis of the distribution of the concrete temperature was performed with the FEM using the COMSOL™ Multiphysics program [32].

Input data for this analysis were the dielectric constant (obtained by using a portable network analyzer [18]), loss factor (fixed at the initial state before applying MW), electromagnetic field, and

heat transfer characteristics (listed in Table 1).

3.3. Results of simulation of electromagnetic field and heat generation within horn antenna during MW heating

The distributions of the electric field (V/m) and temperature (°C) during the application of MWs to the adjusted horn cavity for 15 min (900 s) were determined under the following conditions:

- (Size 1) The horn size was 236.0 mm (width) × 320.1 mm (length) × 150.6 mm (height), and the highest temperature was less than 80 °C (Fig. 3).
- (Size 2) The horn size was 216.7 mm (width) × 333.7 mm (length) × 273.0 mm (height), and the highest temperature was close to 80 °C (Fig. 4).
- (Size 3) The horn size was 236.7 mm (width) × 320.1 mm (length) × 181.2 mm (height), and the highest temperature was greater than 80 °C (Fig. 5).

In size 1 (with the height of the horn adjusted), the electric field was 2.77×10^4 V/m, as presented in Fig. 3(a). The electric field was similar when the height of the horn was increased from 150.6 mm to 273.0 mm (size 2), with an electric distribution of 2.70×10^4 V/m, as presented in Fig. 4(a). In contrast, a decrease in the height from 273.0 mm to 181.2 mm (size 3) provided an electric distribution of 2.69×10^4 V/m. Under the assumption that the temperature of a MW-cured concrete workpiece should not exceed 80 °C, the results indicated that increasing the horn height by λ/4, λ/2, or λ (Figs. 3–5) would produce temperatures of 58.7 °C (Fig. 3(b)), 78.5 °C (Fig. 4(b)), or 90.8 °C (Fig. 5(b)), respectively. When the horn height was increased by λ to achieve a height of 273 mm (Fig. 5(a)), the thermal distribution on the concrete surface was not improved. The thermal distribution became less even, and the hot and cold spots did not decrease significantly in size (Fig. 4).

4. Experiments

4.1. Materials

Type 1 hydraulic Portland cement was used throughout this test. Its chemical composition and physical properties are listed in Table 2. Tap water with a pH of 7.0 and river sand with a fineness modulus of 2.58 and gradation conforming to ASTM C 33 [37] were mixed in specific proportions. The proportions of the concrete material mixed during preparation of the workpiece for testing are listed in Table 3.

4.2. Equipment

For the MW curing, a mobile MW-curing unit for concrete curing was constructed based on the results of the coupled MW thermal analysis, as presented in Fig. 6. The applied MW frequency was 2.45 GHz, with the MWs created by a horn equipped with a magnetron source. Power was set at 800 W to produce MW energy. To control movement and on-off operation, an open wall-mounted programmable logic controller (PLC) was applied with the following specifications: AC receiving power of 100/110/120 V AC (50/60 Hz), 200/220/240 V AC (50/60 Hz), wide-range power voltage fluctuation of 85–264 V AC, operating ambient temperature of 0–55 °C, and insulation resistance between the AC external terminal and case ground (FE) terminal of 20 MΩ or more. The length of the rail was 2.5 m. A 90-W AC motor was installed to drive the device, along with a chain and gears (13 pieces with a gear ratio of 1:5). The motor drive speed was 5 rpm.

To compare the MW curing performance, autoclave curing was carried out. Samples were cured in an autoclave chamber at a maximum temperature of 150 °C at a rate of 75 °C per hour. As shown in Fig. 7, this apparatus includes a heat pump, chromalox precision electric boiler (model CHPES-036AOF10-203), pump

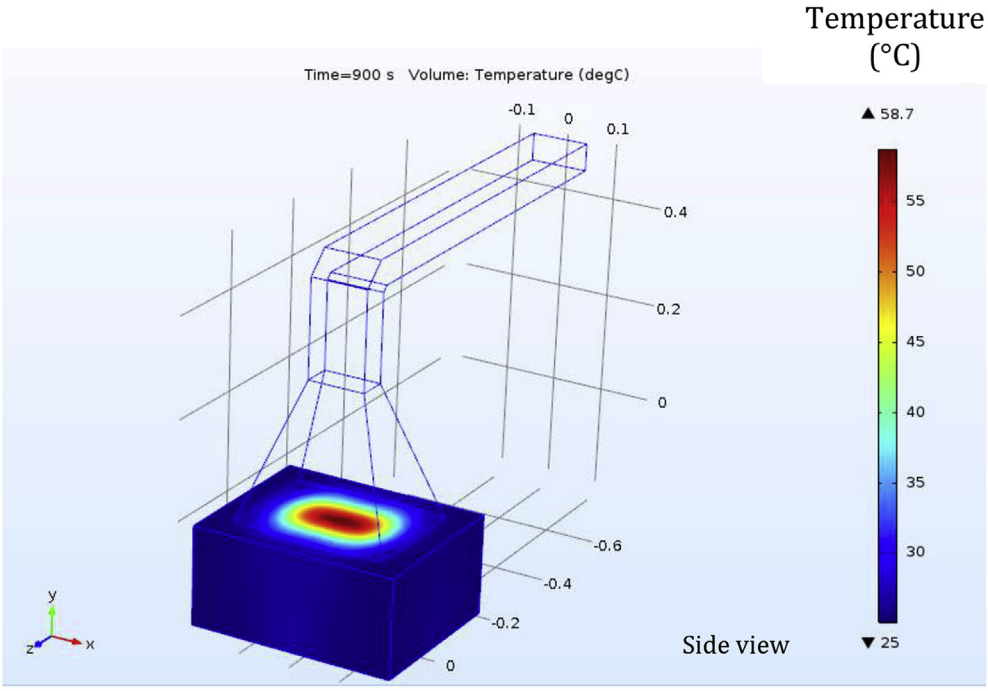

Fig. 3. Temperature of adjusted horn cavity with 236.0 mm width × 320.1 mm length × 150.6 mm height with MW application time of 15 min and highest temperature of less than 80 °C.

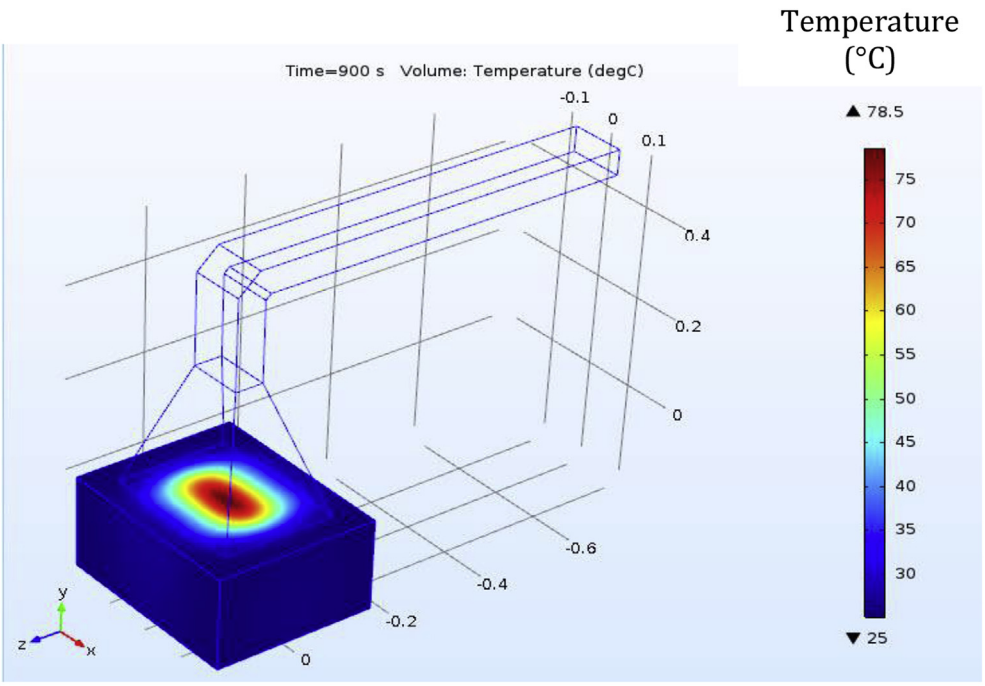

(b) Temperature distribution at surface of concrete workpiece

Fig. 4. Temperature of adjusted horn cavity with 216.7 mm width × 333.7 mm length × 273.0 mm height with MW application time of 15 min and highest temperature close to 80 °C.

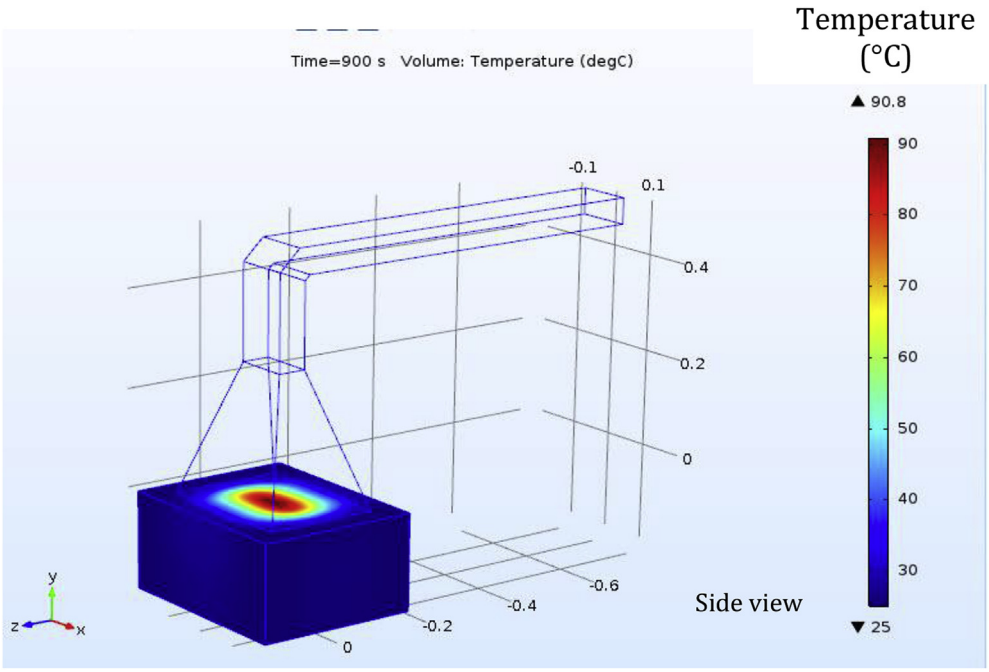

Fig. 5. Temperature of adjusted horn cavity with 236.7 mm width × 320.1 mm length × 181.2 mm height with MW application time of 15 min and highest temperature of greater than 80 °C.

circuit with a 0.75–hp motor, and chamber (serial number: 257835-36225). A microcomputer with a feedback temperature control program was used to control the heat inlet and therefore, the temperature within the chamber.

4.3. Workpiece preparation

Tests were conducted to determine the temperature increase, compressive strength development, and shrinkage values of two groups of 118 cubical workpieces (150 × 150 × 150 mm^3), as

Table 2
Chemical compositions and physical properties of type 1 Portland cement.

Chemical composition (% by mass)	SiO_2	Al2O3	Fe_2O_3	CaO	MgO	K_2O	Na_2O	SO_3	Free CaO
Type 1 Portland cement	20.8	5.22	3.20	66.2	1.24	0.22	0.10	2.41	0.99
Physical properties									
Loss on Ignition (%)		0.19							
Moisture Content (%)		0.53							
Blaine Surface Area (cm^2/g)		3200							
Fineness (Particle Size, % Retained)		0.50							
≥75 μm		5.25							
75 μm		3.60							
45 μm		90.62							
≤36 μm									
Fineness (Retained) on 45 μm (No. 325)		5.75							
Water Requirement (%)		100							
Bulk Density (kg/l)		1.03							
Specific Gravity		3.15							

Table 3
Mixture proportion of concrete (per m^3 of concrete).

Type 1 Portland cement (kg)	Water (kg)	Fine aggregate (River sand) (kg)	Coarse aggregate (Crushed limestone rock) (kg)	Water–cement ratio (by mass)
375	187.5	835	1165	0.50

Fig. 6. Autoclave curing machine.

specified in British standard BS 1881: Part 3 [38]. A constant water-cement ratio of 0.50 was maintained throughout the test. The concrete was placed in a plastic mold, which was then wrapped in a plastic sheet to prevent water evaporation from the concrete.

4.4. Cases used to study autoclave and MW curing

In this study, concrete curing was tested via an autoclave method and MW curing in movement modes. The conditions under which the curing took place are presented in Table 4. The details of each experiment are as follows:

- **Case A:** Concrete subjected to autoclaving for 180 min

Under autoclave curing, concrete workpieces were placed into the cavity after having been mixed for 180 min under conditions

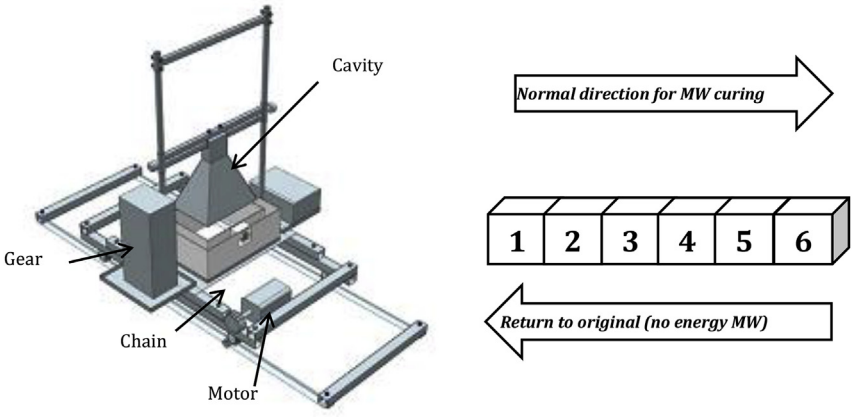

Fig. 7. Prototype for moving mode MW curing and flow diagram for MW concrete curing process (movement steps).

Table 4
Cases and conditions for concrete curing.

Case	MW power (W)	Delay time condition (min)	Heating time (min)	Total time
Case A	Autoclave	After mixing	180	3 h, 8 h, and 1, 3,7, 28 days
Case M1	800	After mixing	45	0, 15, 30, 45, 60, 75, 90 min
Case M2	800	30	45	0, 15, 30, 45, 60, 75, 90 min
Case M3	800	After mixing	30	0, 15, 30, 45, 60, 75, 90 min
Case M4	800	30	30	0, 15, 30, 45, 60, 75, 90 min
Case M5	800	After mixing	15	0, 15, 30, 45, 60, 75, 90 min
Case M6	800	30	15	0, 15, 30, 45, 60, 75, 90 min

whereby the initial temperature of 25 °C was increased until reaching a maximum temperature of 150 °C. The starting time of the autoclave curing was immediately after the concrete was mixed (a delay time of 0 min). After that, the concrete workpieces were cured by wrapping them in plastic for respective periods of 8 h, 1 day, 3 days, 7 days, and 28 days. Finally, their compressive strength and shrinkage values were tested.

- **Case M1:** Concrete subjected to MW curing using 800 W of power for 45 min

The concrete was cured using 800 W of continuous MW power and tested at 15, 30, 45, 60, 75, and 90 min, and at 8 h, 1 day, 3 days, 7 days, and 28 days. The starting time of the MW curing was immediately after the concrete was mixed (a delay time of 0 min).

- **Case M2:** Concrete subjected to MW curing using 800 W of power for 45 min

The concrete was cured using 800 W of continuous MW power for 45 min and tested at 15, 30, 45, 60, 75, and 90 min, and at 8 h, 1 day, 3 days, 7 days, and 28 days. The starting time of the MW curing was 30 min after the concrete was mixed (a delay time of 30 min).

- **Case M3:** Concrete subjected to MW curing using 800 W of power for 30 min

The concrete was cured using 800 W of continuous MW power and tested at 15, 30, 45, 60, 75, and 90 min, and at 8 h, 1 day, 3 days, 7 days, and 28 days. The starting time of the MW curing was immediately after the concrete was mixed (a delay time of 0 min).

- **Case M4:** Concrete subjected to MW curing using 800 W of power for 30 min

The concrete was cured using 800 W of continuous MW power for 30 min and tested at 15, 30, 45, 60, 75, and 90 min, and at 8 h, 1 day, 3 days, 7 days, and 28 days. The starting time of the MW curing was 30 min after the concrete was mixed (a delay time of 30 min).

- **Case M5:** Concrete subjected to MW curing using 800 W of power for 15 min

The concrete was cured using 800 W of continuous MW power and tested at 15, 30, 45, 60, 75, and 90 min, and at 8 h, 1 day, 3 days, 7 days, and 28 days. The starting time of the MW curing was immediately after the concrete was mixed (a delay time of 0 min).

- **Case M6:** Concrete subjected to MW curing using 800 W of power for 15 min

The concrete was cured using 800 W of continuous MW power for 30 min and tested at 15, 30, 45, 60, 75, and 90 min, and at 8 h, 1 day, 3 days, 7 days, and 28 days. The starting time of the MW curing was 30 min after the concrete was mixed (a delay time of 30 min).

As shown in Fig. 7, the movement of the mobile MW-curing unit using motor drive throughout the railway for the distance of 2.5 m with a velocity of 15 m/s. There were six workpieces, each of which was cured using MW energy for 180 min.

4.5. Testing methods

4.5.1. Temperature measurement

Internal and external temperatures of the concrete workpieces were measured. The measurement process began with the use of a laser temperature gun (Fluke 568) having a temperature range of −40 to 650 °C (−40 to 1202 °F). Three concrete levels, top, middle, and bottom, were measured for 15, 30, and 45 min, respectively, at 1 cm from the top surface (top), 7.5 cm from the top surface (middle), and 14 cm from the top surface (bottom), as presented in Fig. 8. Natural heat advection was assumed at the top surface because the wall side was insulated with 10-mm-thick acrylic. In addition, temperature distributions at top and wall surfaces of all cases were detected by a thermo-infrared camera (FLIR C2), which was equipped with a pocket-sized thermal camera designed for a wide range of material and building applications.

4.5.2. Compressive strength test

The respective compressive strengths of the concrete workpieces subjected to autoclave and MW curing were tested using a compressive strength apparatus in accordance with the BS 1881 [38] at 8 h, 1 day, 3 days, and 28 days.

Its compressive strength—the maximum stress that concrete can bear before cracking—is the most important property of concrete. The respective processes for testing the compressive strength of concrete workpieces subjected to autoclave curing, and MW curing were carried out.

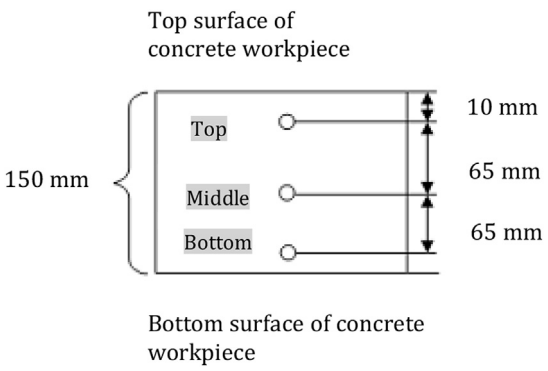

Fig. 8. Installation of temperature measurement system for internal temperature of concrete.

4.5.3. vol stability test

The mass loss, ultimate shrinkage strain, and reduction in shrinkage were tested to determine the volume stability.

The mass loss was assumed the result of a loss of moisture and was measured by first determining the weight of the mixed concrete cubic workpiece as the initial weight of the concrete workpiece. After that, each workpiece was wrapped and sealed in a plastic bag and kept at a temperature of 25 ± 2.0 °C for 12 h. Then, the concrete was weighed to determine the final weight. Further, the moisture loss of the concrete could be calculated using Eq. (5):

$$\text{Moisture loss } (\%) = \left(\frac{W_a - W_b}{W_a}\right) \times 100, \quad (5)$$

where W_a is the initial weight of the concrete before curing (kg), and W_b is the final weight after curing (kg).

For the concrete shrinkage test, after curing using the autoclave or MWs, demountable mechanical (DEMEC) gauges were used to measure the drying shrinkage strain of the concrete. Before testing, six DEMEC gauges were glued to the six sides of each concrete workpiece, with a spacing of 100 mm. Each digital DEMEC strain gauge incorporated a digital indicator with a resolution of 0.0001 mm. During the shrinkage tests, the concrete workpieces were wrapped in plastic sheets and kept in a control room that could be maintained at approximately 25 ± 2 °C, with a relative humidity of 60± 5%. The ultimate shrinkage strain (με) could be calculated by determining the expansion/contraction distances between the DEMEC gauge pairs located on each side of each of the 10 concrete workpieces and averaging the results.

5. Results and discussion

This section presents the results of the thermal behavior of the MW-cured concrete, along with the thermal distribution on the concrete surface and mass loss after MW curing. The compressive strengths of the MW-cured concrete workpieces are also compared to those of the autoclave-cured concrete.

5.1. Effects of application time of MW curing (cases M1, M3, and M5)

Fig. 9 presents the effects of the MW curing of concrete with a water–cement ratio of 0.50, under 800 W of power, and a 45 min curing time (case M1), 30 min curing time (case M2), and 15 min curing time (case M5). It was found that the temperature of the concrete increased continuously. Heating is fastest at the beginning of MW curing because the loss factor is higher when water is present, in accordance with MW heating theory [1]. For case M1, the temperature level increased after 90 min, and the maximum temperature reached 158.5 °C at the top side of the concrete workpiece. In contrast, for cases M3 and M5, when MW curing was stopped after 30 and 15 min, respectively, the temperature was constant because of the reduced moisture content at the concrete surface. This result was due to the fact that the dielectric property (dielectric constant and loss factor) of concrete is strongly related to the moisture level inside the workpiece. This moisture level was low, even though the internal void structure of the concrete meant that excess water was present (i.e., free water remained after the cement particles were hydrated). At the beginning of the MW curing process, the moisture content in the concrete had a direct effect on the temperature because of the high loss factor of the concrete. As a result, the temperature within the concrete increased quickly and unceasingly. Nevertheless, the decreasing moisture content in the concrete also reduced the dielectric property, which meant the temperature of the concrete approached a constant level.

5.2. Effects of delay time for MW concrete curing (comparing cases M1 and M2, M3 and M4, and M5 and M6)

This section discusses the effects of the delay time. Basically, the delay time was the time that elapsed after mixing, before the application of MW energy. The delay time comprised the dormant period, during which the hydration reaction slowed down; the initial setting time, during which the mix began to take on a form; and the final setting time to reach the point at which the structure had formed. Specific delay times are expected to affect various properties in particular ways. For example, if MWs were applied at the final setting time, the pore content would be expected to increase, which would cause the occurrence of microcracking in the paste to be cured.

When considering the effects of the different delays (0 min or immediately after mixing and 30 min), as shown in Fig. 9(a) and (b), it is found that the temperature rise at every temperature measurement point (top, middle, and bottom) with the 30 min delay time is less than that in the case of zero delay time. For instance, a comparison of cases M1 and M2 shows that the temperature increases in the concrete workpiece at the top, middle and bottom positions decreased to 128.5, 109.5, and 97.5 °C with the increase in the delay, respectively. This was because of the high water content, especially the free water content within the concrete workpiece. Because of the high water content, the sample with a delay time of 0 min was able to absorb a large amount of energy and convert it easily into heat [33], whereas at a delay time of 30 min, the cement particles absorbed a large amount of water. Thus, the amount of free water in the workpiece was less than the initial water content.

5.3. Internal thermal distribution on concrete surface

The internal temperature of the concrete after MW curing (M1–M6) was measured at the surface of each concrete workpiece. The MW energy was converted into heat while the temperature increased, as shown in Figs. 10 and 11. The external temperatures at the top surfaces and sides of the concrete workpieces were detected using an infrared camera, which is a non-contact device used to detect infrared heat and convert it into an electronic signal. The temperature distribution results indicated that heat was evident in the concrete wall at a depth of 100–150 mm from the top surface, which was first subjected to the MW irradiation.

As shown in Fig. 10, the temperature distributions at the top concrete surfaces of the concrete workpieces differed according to MW curing times used: 30 min (M1), 30 min (M3), and 15 min (M5). Case M5 had two heating zones, which showed the non-uniformity of the heating. As a result, a high rate of moisture evaporation could occur at the high-temperature zone, while the cooler zone tended to have a low rate of moisture evaporation. This non-homogenous distribution affected the uniformity of the strength development due to the non-uniformity at the top surface of the concrete. This result was seen by the variation in the compressive strength of the concrete with 15 min of MW curing. When the MW curing time was 30 min (M1 and M3), the hot zone had good uniformity, which resulted in a uniform compressive strength for the concrete.

The results on the wall side were similar to those for the top surface. When the MW application time was increased, the compressive strength of the concrete workpiece was more uniform than that of a workpiece with a short MW curing time. In addition to the results shown in Fig. 11, when the delay time was increased (M2, M4, and M6), the trends for the internal thermal distributions of the concrete top surface and wall side were similar to those for

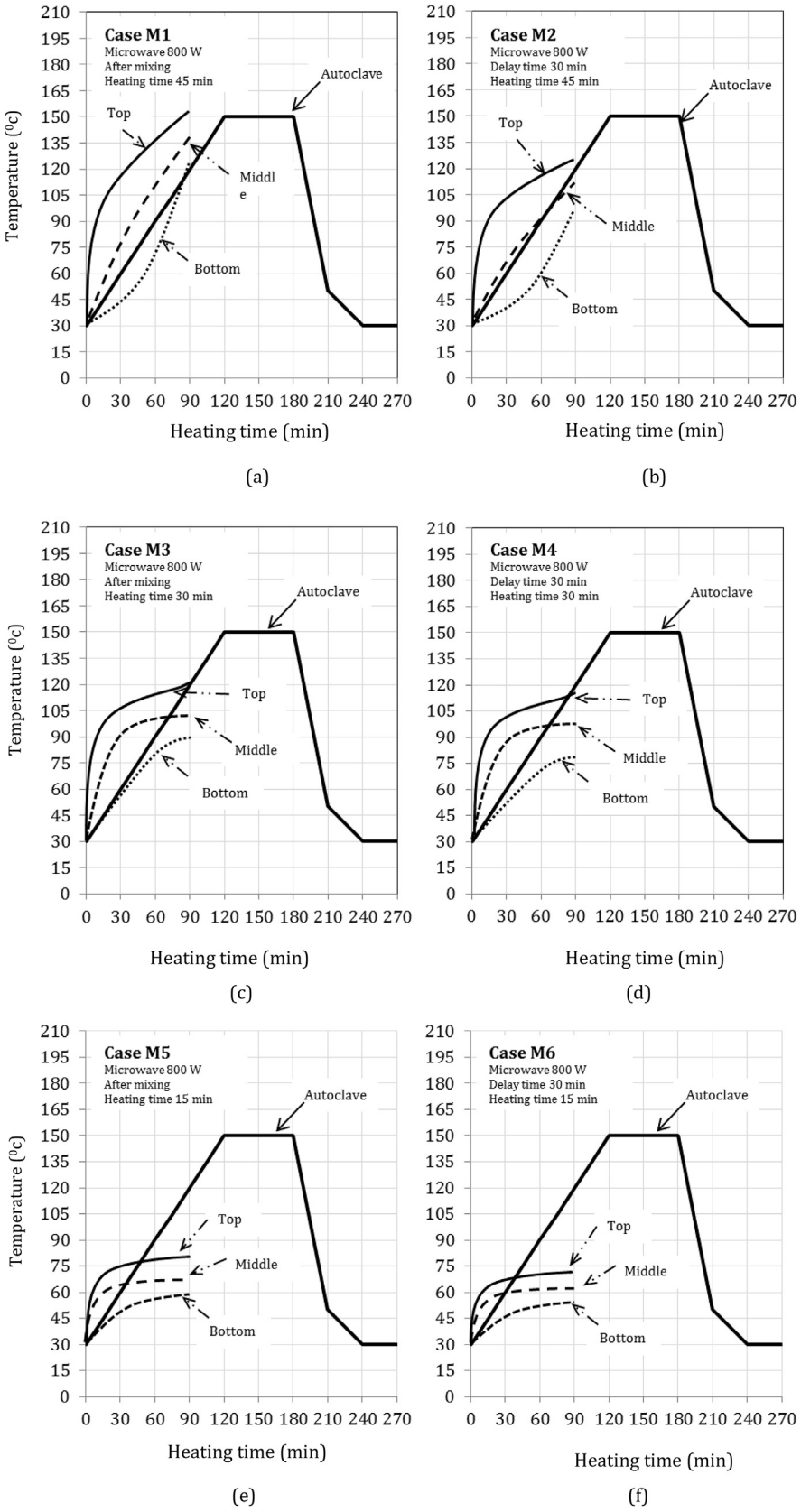

Fig. 9. Temperature profiles of MW-cured concrete during MW curing at 800 W of power: (a) case M1, (b) case M2, (c) case M3, (d) case M4, (e) case M5, and (f) case M6 compared to autoclave curing. Temperature profiles of MW-cured concrete during MW curing at 800 W of power: (a) case M1, (b) case M2, (c) case M3, (d) case M4, (e) case M5, and (f) case M6 compared to autoclave curing.

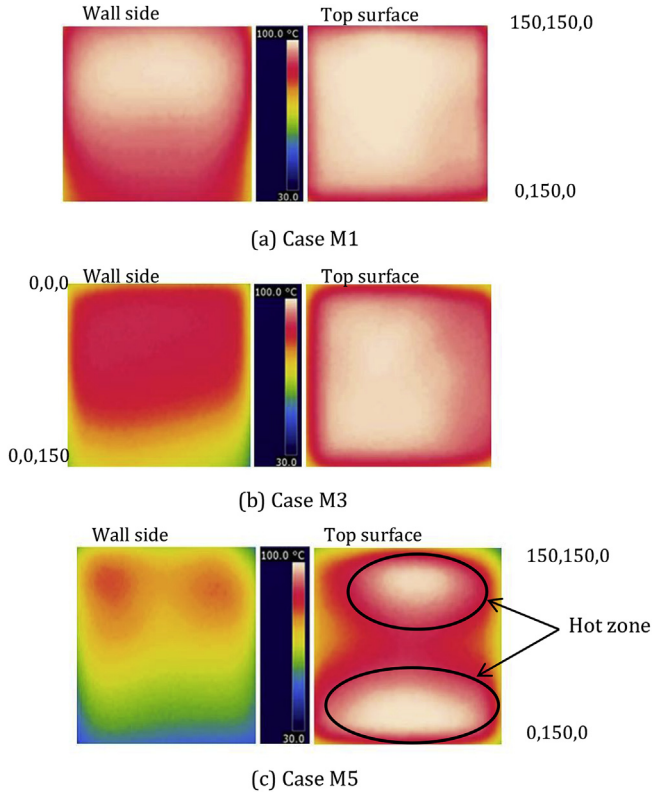

Fig. 10. Temperature distributions at top surface and wall side of cases M1, M3, and M5 after MW curing at 800 W.

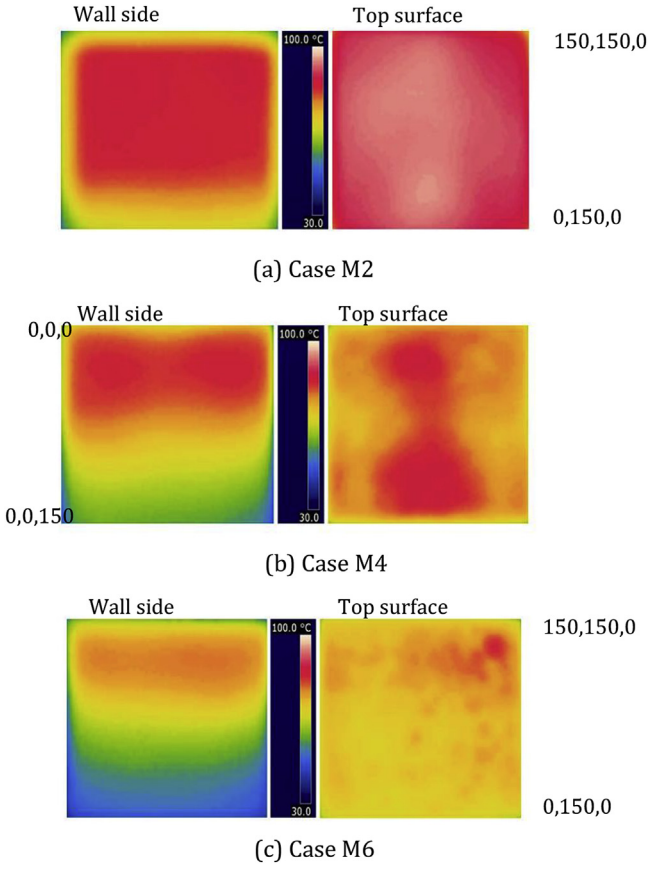

Fig. 11. Temperature distributions at top surface and wall side of cases M2, M4, and M6 after MW curing at 800 W.

cases M1, M3, and M5.

Comparison of the temperature distribution results revealed similarities between cases M1 and M2 and between cases M3 and M4 (Figs. 10 and 11). All four cases had a low rate for the hydration reaction of cement. Thus, when MW was applied to cure the material, no difference in heating state or loss of water occurred inside the concrete workpiece. The shape of the heating curve for the middle of the sample was similar in all four cases. However, the curve for the bottom of the sample was essentially linear in cases M1 and M2, whereas it was exponential in cases M3 and M4. This discrepancy occurred because of the difference in heating time between cases M1 and M2 (45 min) and cases M3 and M4 (30 min). Heating time is related to the movement and number of remaining water molecules at the bottom of concrete workpiece. More water will be lost with a longer MW heating time. When a small number of water molecules remain in the workpiece, the lower MW heating rate and MW penetration depth [1] will result in a heating curve that is uniformly linear. When MW is applied for a shorter time (as in cases M3 and M4), more water molecules will remain at the bottom of workpiece and will react with the MW, resulting in an exponential response of the heating curve [32].

5.4. Performances of MW curing and autoclave curing (cases A and M1–M6)

5.4.1. Moisture loss

In this experiment, the initial water–cement ratio was 0.50 for all the cases (cases A and M1–M6). The water or moisture content in concrete makes it a dielectric material capable of absorbing MW energy and converting it into heat [33]. The moisture losses at the end of the autoclave and MW processing compared with the initial water–cement ratio of 0.50 are presented in Table 6. It can be found that, in all the cases, the moisture content of the concrete rapidly decreased at the final stage of the autoclave or MW curing. It is well known that the moisture content and distribution are strongly related to the porosity, vertical and horizontal transfer of moisture within the concrete workpiece, hydration reaction, etc. At the beginning of the MW process, accumulated moisture from gravitational sedimentation can absorb MW energy, which is partially converted into heat energy. Once the evaporation point is reached, moisture is removed. The concrete permittivity and loss factor are affected by the reduction in moisture and conversion rate for MW curing.

The results listed in Table 5 show that MW curing for 45 min could induce a greater moisture loss in a concrete workpiece than autoclave curing. This was because when MWs were continuously applied to a concrete workpiece, they could elevate the temperature within the concrete, which led to a high amount of accumulated heat and accelerated the moisture evaporation from the inside outward. Conversely, in the autoclave curing, the heat was transported into the concrete, and the low heat conductivity of the concrete produced a low moisture transport.

5.4.2. Compressive strength development

It is generally accepted that the strength of concrete, particularly during the early-age stage, is affected by the water–cement ratio (w/c), temperature, cement type, and curing method. In particular, curing is the process by which hydraulic-cement concrete matures and becomes hard over time [39]. This process ensures that the degree of hydration is sufficient to reduce porosity enough to achieve the desired properties in the concrete.

Table 5
Mass loss and shrinkage of autoclave-cured (case A) and MW-cured concrete (M1–M6).

Case	Parameters indicating volume stability (Mean ± Standard deviation)		
	Mass loss, (%)	Ultimate shrinkage strain (με)	Reduction in shrinkage strain (%)
Case A	3.09 ± 0.25	720 ± 23	−0.48 ± 0.05
Case M1	8.35 ± 1.25	930 ± 14	−0.62 ± 0.07
Case M2	6.23 ± 0.77	830 ± 13	−0.55 ± 0.01
Case M3	5.24 ± 0.24	710 ± 10	−0.47 ± 0.01
Case M4	3.87 ± 0.51	620 ± 12	−0.41 ± 0.03
Case M5	4.78 ± 0.65	530 ± 24	−0.35 ± 0.04
Case M6	3.51 ± 0.88	430 ± 14	−0.29 ± 0.05

Note: Each value reported is the averaged value of the ten workpieces tested.

of the concrete workpiece gradually increases when the age of the concrete increases.

5.4.3. Volumetric stability: drying shrinkage

As previously mentioned, when an outward mass loss (moisture) occurs in a concrete workpiece, it will consequently affect the volume stability and is indicated by drying shrinkage. Hereby, the ultimate drying shrinkage and reduction in drying shrinkage strain were detected using DEMEC gauges. The results are shown in Table 5. It was found that with 45 min of MW curing (M1 and M2), the ultimate drying shrinkage and reduction strain were higher than those for the autoclave curing method. This was consistent with the moisture loss and meant that a high drying shrinkage of

Table 6
Compressive strengths of concrete subjected to autoclave-curing (case A) and MW curing (M1–M6).

Case	Compressive strength (Mean ± Standard deviation) (kg/cm^2)				
	8 h	1 day	3 day	7 day	28 day
Case A	142.14 ± 8.17	236.75 ± 12.23	273.90 ± 13.29	322.50 ± 14.14	386.28 ± 14.32
Case M1	146.25 ± 3.35	241.45 ± 7.24	296.19 ± 8.04	333.21 ± 10.11	322.52 ± 12.95
Case M2	160.02 ± 5.53	255.90 ± 8.19	306.61 ± 12.01	345.88 ± 16.01	349.29 ± 16.29
Case M3	106.32 ± 1.19	224.56 ± 9.21	259.04 ± 10.28	314.92 ± 13.98	344.21 ± 15.12
Case M4	111.65 ± 4.24	239.45 ± 6.65	267.20 ± 9.29	325.80 ± 10.88	355.01 ± 14.10
Case M5	99.15 ± 14.16	190.56 ± 16.27	231.55 ± 15.14	288.23 ± 18.12	340.09 ± 22.11
Case M6	101.12 ± 15.33	196.21 ± 17.61	256.45 ± 12.89	308.13 ± 20.09	360.26 ± 24.22

In this experiment, the results for two types of concrete were considered: the autoclave curing case (case A) and MW curing case (cases M1–M6), as listed in Table 6. The experimental results indicated that the concrete's compressive strength increased rapidly in the first three days when subjected to either autoclave or MW curing. In particular, at 8 h, the compressive strengths of the concrete workpieces subjected to MW energy curing were higher than that of the autoclave workpiece. For example, that of case A was 142.14 ksc, while cases M1 and M2 had compressive strengths of 146.25 and 160.02 ksc, or 2.9% and 12.6% higher, respectively. This was the result of the higher rate of heat generation in the MW curing method compared to the autoclave method.

The strength development values at 8 h for cases M3–M6 were lower than that of case A (autoclave curing). However, in the first 15 min of curing, the temperature rise was equal to 78.5 °C under MW curing for all of the cases (M1–M6). This indicated that increasing the MW curing time to more than 15 min directly affected the strength development. Nonetheless, the strength development rates for cases M3–M6 were lower than that for the autoclave case. This was because of the low heating rate for M3–M6 compared to the autoclave curing.

When considering the short-term strength (28-day compressive strength), which is a main and practical design parameter for concrete engineering, it was found that all of the cases of MW curing had lower values than that of the autoclave curing. This indicated that the MW curing affected the design-day strength or long-term strength. This was due to the inherent thermal insulation of the concrete and its yield of non-uniform hydration products, which caused different temperatures to occur in the processed concrete under high-temperature (MW) curing.

Regarding the compressive strength variation of the MW-cured concrete compared to autoclave-cured concrete, Table 6 also shows that the strengths of the autoclave-cured concrete vary from ±8.2 to ±14.3 ksc or 5.7% (8 h testing age) to 3.7 (28 day testing age). However, those of the MW-cured concrete (M1) vary from ±3.35 to ±12.95 ksc or 2.3% (8 h testing age) to 4.2 (28 day testing age). Based on the overall tendency of MW curing, the strength variation MW-cured concrete occurred with a high moisture loss as a result of a long MW application time. Similarly, cases M2–M6, which had low moisture losses, had lower shrinkages than the autoclave-cured concrete.

6. Concluding remarks

In this work, a horn antenna design was modeled, and performance-related experiments were conducted to investigate the accelerated MW curing of concrete. The following conclusions can be drawn.

- The constructed mathematical models were useful to evaluate the heat generation within a horn-shaped MW cavity at an operating frequency of 2.45 GHz and a MW power of 800 W. The 216.70 mm wide × 333.68 mm long × 273.0 high horn antenna produced a uniform thermal distribution in a concrete workpiece.
- Under the concept of an allowable maximum temperature of not more than 80 °C, the appropriate delay time was 30 min, and applying MW energy for 45 min could improve the maximum 8-h early-age compressive strength of the MW-cured concrete.
- In MW curing with a 45 min application time, the ultimate drying shrinkage and reduction strain were higher than those of the autoclave curing method.
- MW curing is an innovative high performance curing method for concrete at an early stage. However, the long-term performance and durability of MW-cured concrete should be extensively investigated.

Acknowledgments

The authors gratefully acknowledge the Thailand Research Fund under the TRF contract Nos. TRG5780255 and, RTA5680007 and the National Research Universities Project of the Higher Education Commission for supporting this research.

References

[1] A.C. Metaxas, Microwave Heating. Journal of Microwave Power and Electromagnetic Energy, 1991, pp. 237–247.
[2] T. Basak, Role of resonance on microwave heating of oil–water emulsions, AIChE J. 50 (2004) 2659–2675.
[3] Z. Feiyang, C. Shu, X. Guohua, W. Fengwu, Y. Nian, L. Rui, W. Xiaodong, Preparation and bioactivity of apatite coating on Ti6Al4V alloy by microwave assisted aqueous chemical method, Ceram. Int. 42 (2016) 18466–18473.
[4] P.G. Alexander, Emergence of traveling wave endothermic reaction in a catalytic fixed bed under microwave heating, Energy 119 (2017) 989–995.
[5] P. Perre, I.W. Turner, Microwave drying of softwood in an oversized waveguide: theory and experiment, AIChE J. 43 (10) (1997) 2579–2595.
[6] M. Regier, H. Schubert, Microwave processing, in: The Microwave Processing of Foods, Woodhead Publishing, Sawston, Cambridge, USA, 2001.
[7] D.N. Francesca, T. Rosanna, S. Sabina, P. Andrea, B. Gino, A comparison among different instrumental approaches for bromide analysis in foodstuffs digested by a suitably modified microwave procedure, Talanta 60 (2003) 653–662.
[8] C.J. Budd, A.D.C. Hill, A comparison of models and methods for simulating the microwave heating of moist foodstuffs, Int. J. Heat Mass Transf. 54 (2011) 807–817.
[9] C. Emilie, C. Rachida, Z. Julie, G. Thierry, N. Laurent, Simultaneous determination of 31 elements in foodstuffs by ICP-MS after closed-vessel microwave digestion: method validation based on the accuracy profile, J. Food Compos. Analysis 41 (2015) 35–41.
[10] A. Canan, T.Ç. Semra, Identification of irradiated foodstuffs using ESR microwave saturation, Appl. Radiat. Isotopes 122 (2017) 14–20.
[11] X. Shi, X. Shaomei, S. Bo, Z. Jiwei, Microstructure evolution and energy storage properties of potassium strontium niobate boroaluminosilicate glass-ceramics by microwave crystallization, J. Eur. Ceram. Soc. 36 (2016) 4071–4076.
[12] N.U. Avanoor, K.S. Elattuvalappil, R. Ravendran, Crystal structure and microwave dielectric properties of new alkaline earth vanadate A4V2O9 (A = Ba, Sr, Ca, Mg and Zn) ceramics for LTCC applications, Mater. Res. Bull. 88 (2017) 174–181.
[13] N. Afrin, Y. Zhang, J.K. Chen, Thermal lagging in living biological tissue based on non-equilibrium heat transfer between tissue, arterial and venous bloods, Int. J. Heat Mass Transf. 54 (2011) 2419–2426.
[14] E. Simon, L. Pauline, S. Amanda, The possible influence of micro-organisms and putrefaction in the production of GHB in post-mortem biological fluid, Forensic Sci. Int. 139 (2004) 183–190.
[15] W. Xuequan, Microwave curing technique in concrete manufacture, Cem. Concr. Res. 17 (2) (1987) 205–210.
[16] K.Y. Leung, T. Pheeraphan, Microwave curing of Portland cement concrete: experimental results and feasibility for practical applications, Constr. Build. Mater. 9 (1995) 67–73.
[17] P. Rattanadecho, N. Suwannapum, B. Chatveera, D. Atong, N. Makul, Development of compressive strength of cement paste under accelerated curing by using a continuous microwave thermal processor, Mater. Sci. Eng. A 472 (2008) 299–307.
[18] N. Makul, P. Rattanadecho, D.K. Agrawal, Microwave curing at operating frequency of 2.45 GHz of Portland cement paste at early-stage using a multimode cavity: experimental and numerical analysis on heat transfer characteristics, Int. J. Heat Mass Tran. (2010) 1487–1495.
[19] R.G. Hutchison, Thermal acceleration of Portland cement mortars with microwave energy, Cem. Concr. Res. 21 (5) (1991) 795–799.
[20] D. Sohn, D.L. Johnson, Microwave curing effect on the 28 day strength of cementitious materials, Cem. Concr. Res. 29 (1999) 241–247.
[21] Microwave Method and Apparatus for Heating Pavement, by M.R. Jeppson, C. Calif, United States Patent, 425 2 487, 1981.
[22] Concrete Curing Machine, by C.B. Sipherd, J.R. Lease, R.L. Stainbrook, United States Patent 649 7 531 B1, 2002.
[23] N. Makul, Innovative hybrid curing method for accelerating the strength of high-performance cement paste using microwave heating coupling with low-pressure processing, Constr. Build. Mater. 105 (2016) 245–252.
[24] T.R. Neelakantan, S. Ramasundaram, R. Vinoth, Accelerated curing of M30 grade concrete specimen using microwave energy, Asian J. Appl. Sci. 7 (2014) 256–261 (Open Access).
[25] P.S. Mangat, K. Grigoriadis, S. Abubakri, Microwave curing parameters of in-situ concrete repairs, Constr. Build. Mater. 112 (2016) 856–866.
[26] A. Buttress, A. Jones, Sam Kingman, Microwave processing of cement and concrete materials – towards an industrial reality? Cem. Concr. Res. 68 (2015) 112–123.
[27] R. Barbarulo, H. Peycelon, S. Prené, J. Marchand, Delayed ettringite formation symptoms on mortars induced by high temperature due to cement heat of hydration or late thermal cycle, Cem. Concr. Res. 35 (2005) 125–131.
[28] G. Escadeillas, J.-E. Aubert, M. Segerer, W. Prince, Some factors affecting delayed ettringite formation in heat-cured mortars, Cem. Concr. Res. 37 (2007) 1445–1452.
[29] A. Pavoine, X. Brunetaud, L. Divet, The impact of cement parameters on Delayed Ettringite Formation, Cem. Concr. Compos. 34 (2012) 521–528.
[30] J. Bergmans, P. Nielsen, R. Snellings, K. Broos, Recycling of autoclaved aerated concrete in floor screeds: sulfate leaching reduction by ettringite formation, Constr. Build. Mater. 111 (2016) 9–14.
[31] T. Chow Ting Chan, H.C. Reader, Understanding Microwave Heating Cavities, Artech House, Inc., Norwood, MA 02062 USA, 2000.
[32] COMSOL, Inc, COMSOL Multiphysics User's Guide, COMSOL AB, Singapore, 2007, Version 3.4. .
[33] A.C. Metaxas, R.J. Meridith, Industrial Microwave Heating, Peter Peregrinus, Ltd., London, 1983.
[34] P. Rattanadecho, K. Aoki, M. Akahori, Experimental and numerical study of microwave drying in unsaturated porous material, Int. J. Heat Mass Transf. 28 (2001) 605–616.
[35] L.A. Campanone, N.E. Zaritzky, Mathematical analysis of microwave heating process, J. Food Eng. 69 (2005) 359–368.
[36] S. Hauck Harold, Design considerations for microwave oven cavities. IEEE Xplore: IEEE transactions on industry applications, 1979, pp. 74–80.
[37] American Society for Testing and Materials, ASTM C33/C33M – 13 Standard Specification for Concrete Aggregates, vol. 4, Annual Book of ASTM Standards, 02, Philadelphia, PA, USA, 2013.
[38] British Standards Institution, BS 1881, Part 4, Method of Testing Concrete for Strength, 2011. London, United Kingdom.
[39] American Concrete Institute, ACI 318–Building Code Requirements for Structural Concrete and Commentary, 2008. Farmington Hills, MI, USA.